Thermal and Structural Characterization of $(CH_3)_3CCl$

J. Ll. Tamarit,*,† D. O. López,† X. Alcobé,‡ M. Barrio,† J. Salud,† and L. C. Pardo†

Departament de Física i Enginyeria Nuclear, ETSEIB, Universitat Politècnica de Catalunya, Diagonal, 647, 08028 Barcelona, Catalonia, Spain, and Serveis Científico-Tècnics, Universitat de Barcelona Lluís Solé i Sabaris, 1−3, 08028 Barcelona, Catalonia, Spain

Received October 11, 1999. Revised Manuscript Received November 15, 1999

The polymorphism of $(CH_3)_3CCl$ has been further investigated by both thermal and X-ray powder diffraction experiments. From the former, the phase transitions between the different phases (IV, III, II, I, and L) have been thermally characterized, and in particular, the temperature domain of phase II has been settled to be from 217.9 to 219.8 K by means of C_p measurements. The structure of the lowest-temperature phase IV of $(CH_3)_3CCl$ has been determined by X-ray powder diffraction and Rietveld profile refinement. The structure, $P2_1/m$ with two molecules per unit cell, has been found to be isostructural with that of phase II of $(CH_3)_3CCN$. The intermolecular interactions in the solid-state phases for $(CH_3)_3CCl$ as well as for $(CH_3)_3CCN$ have been analyzed by the study of the isobaric thermal-expansion tensor. The anisotropy of such interactions are discussed in the light of the previously studied dynamics disorder.

1. Introduction

2-Chloro-2-methyl-propane, $(CH_3)_3CCl$ or *tert*-butyl-chloride (TBCl), belongs to a group of molecular compounds of common chemical structure, $(CH_3)_3CX$. For a large number of substituents X, the existence of an orientationally disordered phase has been found (X = Br, I, CN, SH, NO_2, CH_3, NH_2, COOH, CH_2OH, and so on).[1−4] Many detailed studies of the molecular motions in the solid phases of *tert*-butyl compounds have been performed using neutron scattering,[5−9] dielectric,[10−13] NMR,[14−21] and, to a lesser extend, X-ray diffraction [22−24] techniques. The results of these measurements have enabled researchers to better characterize the dynamics and the thermodynamics of the ordered and disordered phases. It is then well-known that the order−disorder transitions are associated with the motions of the molecules in the crystal lattice. In particular, the molecular motions present in each phase of *tert*-butyl halides (X = Cl, Br, and so on)[15−20] and X = CN [7,8,14] and SH [18,19] have been largely studied. As far as X = Cl is concerned, differential thermal analysis,[25] NMR,[17−20] dielectric,[10,11] and X-ray powder diffraction studies[22,23] revealed the existence of an extent polymorphism. At 247.8 K, the liquid freezes to an orientationally disordered fcc (face-centered cubic) structure (phase I). Upon further cooling, this phase transforms at about 220 K to an unknown structure (phase II). The stability temperature domain (about 2 K) of this phase has been the subject of several works, and its properties or even more, its existence, remains still an open question. Phase II transforms to a tetragonal ($P4/nmm$)[26] phase III, where uniaxial molecular reorientations about the C−Cl axis (C_3' axis or dipole axis of the molecule) are present.[17,20,27] In addition to this 3-fold rotation, small fluctuations of the dipole axis (a few degrees) are also

* To whom correspondence should be addressed. Tel.: 34 93 401 65 64. Fax: 34 93 401 66 00. E-mail: JOSE.LUIS.TAMARIT@UPC.ES.
† Universitat Politècnica de Catalunya.
‡ Universitat de Barcelona Lluís Solé i Sabaris.

(1) Parsonage, N. G.; Staveley, L. A. K. *Disorder in Crystals;* Clarendon Press: Oxford, 1978.
(2) Urban, S. *Adv. Mol. Relax. Interact. Proc.* **1981**, *21*, 221.
(3) Reuter, J.; Büsing, D.; Tamarit, J. Ll.; Würflinger, A. *J. Mater. Chem.* **1997**, *7*, 41.
(4) Guthrie, G. B.; McCollough, J. P. *J. Phys. Chem. Solids* **1961**, *18*, 53.
(5) Urban, S.; Mayer, J.; Belushkin, A. I. *Acta Phys. Pol., A* **1983**, *64*, 161.
(6) Leadbetter, A. J.; Ward, R. C.; Richardson, R. M. *J. Chem. Soc., Faraday Trans. 2* **1985**, *81*, 1067.
(7) Frost, J. C.; Leadbetter, A.; Richardson, R. M.; Ward, R. C.; Goodby, J. W.; Gray, G. W.; Pawley, G. S. *J. Chem. Soc., Faraday Trans. 2* **1982**, *78*, 179.
(8) Gane, P. A. C.; Leadbetter, A. J.; Ward, R. C.; Richardson, R. M.; Pannetier, J. *J. Chem. Soc., Faraday Trans. 2* **1982**, *78*, 995.
(9) Frost, J. C.; Leadbetter, A.; Ward, R. C.; Richardson, R. M. *J. Chem. Soc., Faraday Trans. 2* **1982**, *78*, 1009.
(10) Wilmers, J.; Briese, M.; Würflinger, A. *Mol. Cryst. Liq. Cryst.* **1984**, *107*, 293.
(11) Urban, S.; Janik, J. A.; Lenik, J.; Mayer, J.; Baluga, T.; Wrobel, S. *Phys. Status Solidi A* **1972**, *10*, 271.
(12) Kreul, H. G.; Waldinger, R.; Würflinger, A. *Z. Naturforsch. A* **1992**, *47*, 1127.
(13) Büsing, D.; Jenau, M.; Reuter, J.; Würflinger, A.; Tamarit, J. Ll. *Z. Naturforsch. A* **1995**, *50*, 502.
(14) O'Reilly, D. E.; Petterson, E. M.; Scheie, C. E.; Seyfarth, E. *J. Chem. Phys.* **1973**, *59*, 3576.
(15) Köksal, F. *J. Chem. Soc., Faraday Trans. 2* **1980**, *76*, 550.
(16) Hasebe, T.; Soda, G.; Chihara, H. *Bull. Chem. Soc. Jpn.* **1981**, *54*, 2583.
(17) Ohtani, S.; Hasebe, T. *Chem. Lett.* **1986**, 1283.
(18) Szczesniak, E. *Mol. Phys.* **1986**, *58*, 551.
(19) Aksness, D. W.; Ramstad, K. *Acta Chem. Scand. Ser. A* **1987**, *41*, 1.
(20) Hasebe, T.; Ohtani, S. *J. Chem. Soc., Faraday Trans. 1* **1988**, *84*, 187.
(21) Hasebe, T. *Bull. Chem. Soc. Jpn.* **1990**, *63*, 2877.
(22) Urban, S.; Domoslawski, J.; Tomkowicz, Z. *Mater. Sci.* **1978**, *4*, 91.
(23) Urban, S.; Tomkowicz, Z.; Mayer, J.; Waluga, T. *Acta Phys. Pol., A* **1975**, *48*, 61.
(24) Jenau, M.; Reuter, J.; Tamarit, J. Ll.; Würflinger, A. *J. Chem. Soc., Faraday Trans.* **1996**, *92*, 1899.
(25) Wenzel, U.; Schneider, G. M. *Mol. Cryst. Liq. Cryst. (Lett.)* **1982**, *72*, 255.
(26) Rudman, R.; Post, B. *Mol. Cryst.* **1968**, *5*, 95.
(27) Goyal, P. S.; Nawrocik, W.; Urban, S.; Domoslawski, J.; Nakaniec, I. *Acta Phys. Pol. A* **1974**, *46*, 399.

10.1021/cm9911565 CCC: $19.00
Published on Web 01/22/2000

present.[20] In the case of phase I of X = CN, these fluctuations are about 10−15°, and in the case of X = Br, large fluctuations of about 30−60° could be found.[6] Concerning the compound X = Cl, the crystallographically uncharacterized lowest-temperature phase IV is reached at 183 K. The molecular motions encountered in this phase IV consist of both uniaxial molecular reorientations (around C_3' axis as in phase III) as well as methyl reorientations (around the C_3 axis, i.e., an axis passing through the parent carbon atom and perpendicular to the plane of the protons). The former motion is faster than the latter.[17,20] The motions around C_3' and C_3 axes are in accord with the dielectric measurements, which indicate that the molecular dipole does not reorient in the lowest-temperature phase.

Although the more studied *tert*-butyl compounds correspond to the *tert*-butyl halides, only the structure of the lowest-temperature ordered phases of X = CN has been determined.[7] The required single crystal for data collection on these phases can be hardly obtained, and powder pattern profile refinement is the only possible approach. In some cases, because of the complexity of the powder pattern and the large number of molecules per unit cell ($Z = 16$ for X = Br[6] or $Z = 7$ for X = CH_2OH[28]), even a profile refinement has not been possible.

On the basis of X-ray powder diffraction measurements, it was proposed early that the pattern of phase IV of TBCl could be indexed as orthorhombic with $Z = 12$ molecules per unit cell, this result being obtained by applying the Louër and Louër method to 23 reflections.[22]

In a recent molecular dynamics simulation,[29] it has been found that the structure of phase IV should correspond to a monoclinic ($P2_1/m$) lattice with cell parameters of $a = 5.99$, $b = 7.21$, and $c = 6.18$ Å and $\beta = 88.7°$.The fractional coordinates of sites in the monoclinic phase were also determined, and as we will describe later, they have been used in the present work as starting points in our profile refinement.

The purpose of the present paper is to report on the polymorphic characteristics of TBCl and more particularly on the structure of phase IV. It will be established with no doubt that phase IV, of particular concern in this paper, is monoclinic ($P2_1/m$). In addition, we examine the relationship between the rotational molecular disorder and the lattice structures for the different phases of the mentioned compound. Comparisons with phases II and I of TBCN will be performed in the light of the analysis of the anisotropy of the isobaric thermal-expansion tensor.

2. Experimental Section

2.1. Materials. TBCl was obtained from Aldrich Chemical Co. with purity higher than 99% (controlled by the analysis of the melting process by means of calorimetric measurements).

2.2. X-ray Powder Diffraction. X-ray powder diffraction data were collected using a horizontally mounted INEL cylindrical position-sensitive detector (CPS-120)[30] equipped with a liquid-nitrogen INEL CRY950 cryostat (80−330 K). The detector (250 mm curvature radius) used in Debye-Sherrer geometry, consisted of 4096 channels, and the angular step was around 0.03° (2θ). Monochromator Cu $K\alpha_1$ radiation was selected with an asymmetric focusing incident-beam curved quartz monochromator. The generator power was set to 40 kV and 30 mA.

The samples were introduced in 0.5 mm diameter Lindemann glass capillaries in the liquid state at room temperature and were rotated around the θ axis during the experiment to help in generating a proper averaging of crystallites. The design of the cryostat was modified in order to measure the temperature by means of a Pt-100 Ω probe in the sample chamber containing the gas (He) as heat exchanger.

External calibration using the cubic phase $Na_2Ca_3Al_2F_4$ was performed to convert channels to degrees (2θ) by means of cubic spline fittings in order to correct the deviation from angular linearity in PSD (position-sensitive detector) according to recommendations.[31,32] DIFFRACTINEL software was used for the calibration and for the peak position determinations after Gaussian fittings in the standard measurements. These were performed at least every 20 K step in the temperature range of phase IV, every 10 K for phase III and every 5 K for the orientationally disordered phase I. Acquisition times were 180 min for patterns of phases IV and III and 90 min for phase I. The slew rate was 1 K min^{-1} with a stabilization time of 10 min at each temperature before data collection.

An additional pattern for phase IV (at 123.2 K) was measured for structure determination and refinement purposes with an acquisition time of 800 min.

2.3. Thermal Analysis. Transition temperatures as well as enthalpy changes were determined by means of a modulated DSC TA2910 system from TA Instruments, Inc., equipped with the cooling accessory. Heating rates of 2 K min^{-1} were used. Samples (about 15 mg) were introduced in high-pressure stainless steel pans from Perkin-Elmer (pan mass about 600 mg) in order to prevent chemical reactions and to avoid undesirable effects on the thermograms due to the high vapor pressure of the compound. Heat capacity (C_p) measurements by using the modulated technique with a period of 40 s, a temperature amplitude of ±0.5 K, and a scanning rate of 0.5 K min^{-1} were performed around the temperature domain of phase II.

3. Results and Discussion

3.1. Thermodynamic Study. As it has been pointed out, TBCl displays four different solid phases at atmospheric pressure, denoted as phases I, II, III, and IV in order of decreasing temperature. An additional phase at high pressure was also found.[10,25] The temperatures and enthalpy changes for the different transitions are gathered in Table 1. Figure 1 displays the cooling and heating differential scanning calorimetric runs at 2 K min^{-1} and, in the inset, a heating run at 0.05 K min^{-1}. The transition III−II is shown as a shoulder on the low-temperature side of the peak corresponding to the II−I transition.

To separate both transitions and to account for the temperatures associated with the III−II and II−I phase transitions, measurements of C_p by means of the modulated technique were performed. In Figure 2, we plot the C_p values obtained around the temperature domain between 210 and 225 K. Such high-resolution C_p measurements enable us to separate both transitions. It must be pointed out that the values of C_p have not

(28) Salud, J.; Barrio, M.; López, D. O.; Tamarit, J. Ll.; Alcobé, X. *J. Appl. Cryst.* **1998**, *31*, 748.
(29) Chen, J.; Bartell, L. S. *J. Phys. Chem.* **1993**, *97*, 10645.
(30) Ballon, J.; Comparat, V.; Pouxe, J. *Nucl. Instrum. Methods* **1983**, *217*, 213.
(31) Deniard, P.; Evain, M.; Barbet, J. M.; Brec, R. *Mater. Sci. Forum* **1991**, *79−82*, 363.
(32) Evain, M.; Deniard, P.; Jouanneaux, A.; Brec, R. *J. Appl. Cryst.* **1993**, *26*, 563.

Table 1. Temperature and Enthalpy Changes for the Phase Transitions of TBCl

phase transition	*T*/K	ΔH (kJ mol^{-1})	reference
IV−III	183.1	1.86	11
	182.9	1.87	33
	182.9 ± 0.3		17
	183.6 ± 0.3	2.08	this work
III−II	217.7 ± 0.3		17
	217.9 ± 0.3		this work
III−II/I	219.4	5.66	11
	219.2	5.88	33
	219.5 ± 0.3		17
	219.8 ± 0.3	5.75	this work
I−L	248.4	1.99	11
	247.5	2.07	33
	248.2 ± 0.3		17
	247.8 ± 0.3	1.89	this work

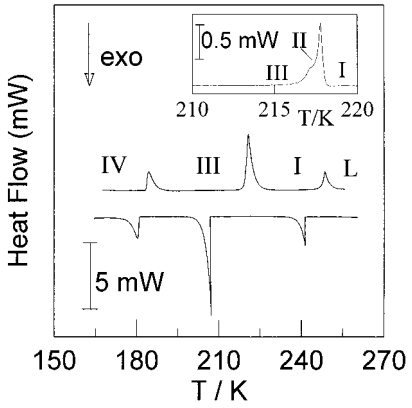

Figure 1. Cooling and heating differential scanning calorimetric traces for TBCl at 2 K min^{-1}. The inset corresponds to a heating run at 0.05 K min^{-1}.

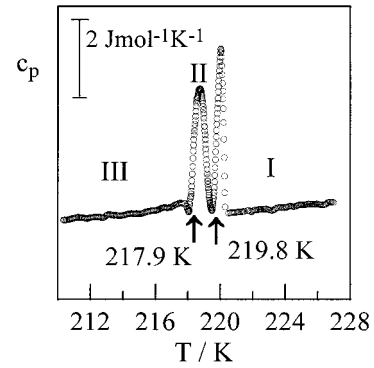

Figure 2. Specific heat (C_p) variation with the temperature around the III−II and II−I transitions.

been quoted due to the large error associated with the high capacity of the sample container, despite the high resolution in the relative values. Such errors, together with the rounding-off effects, do not enable us to quote separately the enthalpy changes associated with the III−II and II−I transitions. As can be seen in Table 1, there is very close agreement between the temperatures of the III−II and II−I transitions determined in this work and the corresponding work of Ohtani and Hasebe.[17]

3.2. Crystallographic Study. *Phase IV.* For indexing purposes, a pattern for phase IV at 123.2 K was obtained with an acquisition time of 800 min. To determine the symmetry of this phase, a data set of the 25 unambiguously defined reflections was indexed by means of the program DICVOL91.[34] A monoclinic cell with reliability indices M(25)[35] and F(25)[36] of 49.4 and 67.1, respectively, was obtained. The final cell parameters, refined using the AFMAIL program,[37] were a = 6.261(2), b = 7.516(2), and c = 6.001(2) Å, β = 92.128(9)°, and V = 282.2(2) Å^3. From density data and volume changes[10] at the phase transitions, the number of molecules per unit cell was determined to be Z = 2.

From the systematic absences, the space group is either $P2_1/m$ or $P2_1$ ((*0k*0) reflections with *k* odd were absent). The former space group corresponds to that obtained by means of molecular dynamics simulations in a relatively recent work.[29] In this work, the fractional coordinates of sites in this monoclinic phase IV were determined, and these have been used as the starting point for a Rietveld refinement with the FULLPROF.98 program.[38] A preliminary standard procedure refining atomic coordinates in the 13−100° 2θ range produced noticeable molecular distortions, indicating that rigid body refinement has to be done. The asymmetric unit required for the refinement was constructed using the properties reported in the vapor phase for the C_{3v} molecule: 1.527 Å for C−C and 1.805 Å for the C−Cl bonds and 107.85° for the C−C−Cl and 111.1° for the C−C−C angles.[39] The 14 parameters refined in the procedure were the following: the overall scale factor; the 2θ-shift of the pattern; the lattice parameters; the center of the asymmetric units X_o and Z_o (Y_o = $^1/_4$, because the mirror plane of the molecule must be coincident with the mirror plane of the space group); one Euler angle (between the molecular *z* axis and the crystallographic *c* axis, the other two Euler angles were fixed according to the same reason as that for the Y_o coordinate); the peak shape parameters *U*, *V*, and *W*; the overall isotropic temperature factor *B*; and the η of the pseudo-Voight function.

The background was interpolated with the help of one acquisition with an empty Lindemann capillary and the comparison with the interpolated background of the sample capillary in order to introduce the matrix effect. The final parameters obtained from the refinement at 123.2 K are gathered in Table 2. The differences from the starting fractional coordinates (see Chen and Bartell[29]) were small and mainly concern the *x* coordinate of the chlorine and the central carbon (C1) atoms. The smallest changes were found to be in the coordinates of the methyl carbon atoms related by the mirror plane (C3 and C4 in Table 3). The collected and calculated profiles are shown in Figure 3, together with the plot difference between them. From such a difference, we can see that the calculated profile matches quite well the observed one. Although the poor signal at high angles and the difficulty in avoiding the preferred orientation make impossible a better refinement, the proposed structure can be considered as completely reasonable according

(33) Dworkin, A.; Guillamin, M. *J. Chim. Phys. Phys.-Chim. Biol.* **1966**, *63*, 53.
(34) Louër, D.; Boultif, A. *DICVOL91 program*; Laboratoire de Crystallochimie, University de Rennes I: Rennes, France, 1991.
(35) De Wolf, P. M. *J. Appl. Crystallogr.* **1968**, *5*, 108.
(36) Smith, G. S.; Snyder, R. L. *J. Appl. Cryst.* **1979**, *12*, 60.
(37) Rodriguez-Carvajal, J. *AFMAIL program;* Laboratoire Leon Brillouin, CEA-CNRS: Gif-Sur-Yvette, France, 1985.
(38) Rodriguez-Carvajal, J. *FULLPROF.98 program*; Laboratoire Leon Brillouin, CEA-CNRS: Gif-Sur-Yvette, France, 1998.
(39) Hilderbrandt, R. L.; Wieser, J. D. *J. Chem. Phys.* **1971**, *55*, 4648.

Table 2. Results from the Profile Refinement of the Low-Temperature Phase IV of TBCl at 123.2 K[a]

parameter	value
overall scale factor	0.0587(5)
2θ-shift (zero correction)	0.008(2)°
lattice parameters	
a (Å)	6.2613(7)
b (Å)	7.5168(8)
c (Å)	6.0064(6)
β (°)	92.124(8)
center of the asymmetric unit (X_o, Y_o*, Z_o)	(0.203, $^1/_4$, 0.798)
Euler angles (ϕ*,θ, ψ*) (°)	(90, 92.2,90)
η of pseudo-Voight function	0.92(2)
peak shape parameters (U, V, W) (Å)	0.12(5), −0.04(3), 0.037(4)
overall isotropic temp. factor (B) (Å^2)	4.3(1)
R_p[b]	4.25
R_{wp}[c]	6.41
R_B[d]	22.4

[a] Parameters marked by * were not refined. [b] $R_p = \sum|Y_o(i) - Y_c(i)|/\sum Y_o(i)$. [c] $R_{wp} = [\sum\{1/y_o(i)\}\{y_o(i) - y_c(i)\}^2/\sum y_o(i)]^{1/2}$. [d] $R_B = \sum_{jref}|I_o(j) - I_c(j)|/\sum_{jref} I_o(j)$.

Table 3. Fractional Atomic Coordinates for Phase IV of $(CH_3)_3CCl$

atom	x	y	z	atom	x	y	z
Cl	0.203	0.250	0.902	H23	−0.113	0.368	0.773
C1	0.203	0.250	0.798	H31	0.237	0.539	0.776
C2	−0.031	0.250	0.709	H32	0.327	0.419	0.540
C3	0.320	0.419	0.723	H33	0.484	0.419	0.796
C4	0.320	0.081	0.723	H41	0.487	0.081	0.787
H21	−0.115	0.130	0.763	H42	0.317	0.077	0.540
H22	−0.034	0.254	0.526	H43	0.238	−0.037	0.787

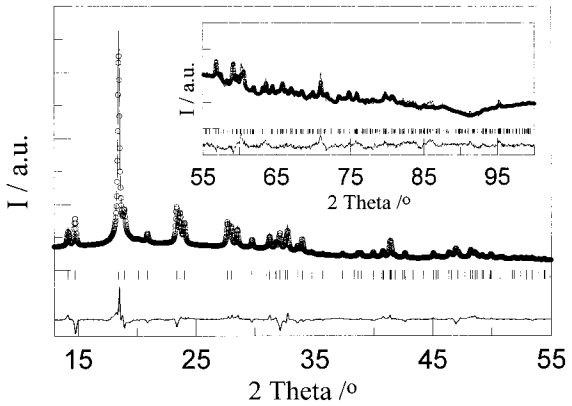

Figure 3. Experimental (○) and theoretical (—) diffraction patterns of phase IV ($P2_1/m$) for TBCl at $T = 123$ K along with the difference profile. The intensity of the inset is magnified 40 times.

to the calculated reliability factors. The fractional atomic coordinates are included in Table 3.

Figure 4 shows the (010) crystallographic plane for TBCl. The molecules are arranged in a head-to-tail configuration in such a way that the C−Cl bond is close to the *c* axis of the lattice. Such a bond, which corresponds to the dipole direction of the molecule, is tilted about 2.2° relative to the *c* in the *ac* plane, a situation that can be compared to that (4°) of the dipole corresponding to the TBCN molecule at 147 K. According to NMR results,[20] the fluctuations of the dipole axis (uniaxial molecular reorientations between identical positions) increase with the increase in temperature. These fluctuations can be assumed, as in the case of TBCN in the lowest temperature phase, as the reason

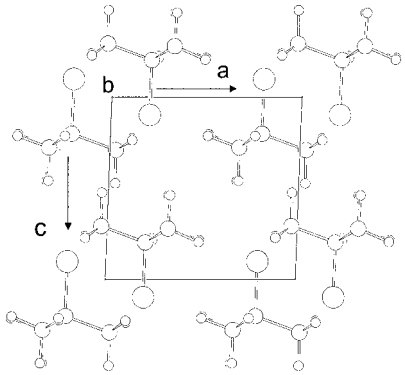

Figure 4. (0*k*0) crystallographic plane of the monoclinic phase IV of TBCl.

to move apart faster the molecules in the *a* crystallographic direction, giving rise to a high variation of this parameter with temperature (see below). Until now, no structure determination of the ordered phases of *tert*-butyl compounds has been reported, with the exception of the TBCN.[7] This analysis shows that the lowest temperature phases of TBCl and TBCN are completely isostructural.

Phase III. Rudman and Post[26] stated that the most probable space group of phase III was $P4/nmm$ with the lattice parameters of $a = 7.08$ and $c = 6.14$ Å and $Z = 2$ at 213.2 K. According to the reported structure, chlorine atom and one carbon atom lie on 4-fold rotation axes parallel to *c* (at $x = y = 0.25$). As the TBCl molecule does not display such an intrinsic symmetry, it must be acquired by means of the rotation about the molecular axis Cl−C, as it has been shown by NMR measurements.[20,21,40]

Phases II and I. Due to the temperature fluctuations (±0.5 K) of the INEL CRY950 cryostat and to the very narrow temperature domain of existence for phase II (1.9 K), it has not been possible to obtain the corresponding pattern. Nevertheless, in one tentative of the performed experiments, a pattern showed the reflections corresponding to the highest temperature orientationally disordered phase I (*fcc*) and that of a tetragonal phase (which matches up the pattern of the tetragonal phase III). That means that the phase II must be also tetragonal. As proposed by Ohtani and Hasebe,[17] phase II should be ordered (as far as the unit cell is concerned) in a way very similar to that of phase III. Nevertheless, the orientational disorder should correspond to the onset of a kind of molecular motion referred to "*as hindered molecular tumbling*", in addition to the methyl reorientation along C_3 axis and the *tert*-butyl reorientation along the dipole axis (C_3' axis).

3.3. Thermal-Expansion Tensor. The anisotropy of the intermolecular interactions in the solid state of TBCl has been shown by means of the isobaric thermal-expansion tensor. Although the thermal-expansion tensor of organic crystals has only been determined in a few cases, it is well-known that some information about the intermolecular interactions can be obtained from it. The deformation of a crystal by a change in the temperature is minimal in the directions of the highest atomic density, i.e., the directions of the highest inter-

(40) Stejskal, E. O.; Woessner, D. E.; Farrar, T. C.; Gutowsky, H. S. *J. Chem. Phys.* **1959**, *31*, 55.

Table 4. Lattice Parameters Corresponding to the Phases IV−I of TBCl together with the Polynomial Equation[a] $p = p_o + p_1T + p_2T^2$ to which They Were Fitted

phase	T	a	b	c	β	parameter	p_o	$p_1 \times 10^3$	$p_2 \times 10^5$	$R \times 10^5$
IV	93.2	6.248(2)	7.501(3)	5.991(4)	92.18(3)	a	6.295(12)	−1.39(18)	0.96(6)	13
	113.2	6.262(2)	7.509(3)	6.002(5)	92.23(3)					
	123.2	6.261(2)	7.516(2)	6.001(2)	92.128(9)	b	7.447(27)	0.53(41)	0.04(1)	25
	133.2	6.280(4)	7.524(4)	6.021(5)	92.24(4)					
	153.2	6.307(4)	7.539(4)	6.035(5)	92.22(3)	c	5.933(18)	0.53(27)	0.09(9)	20
	173.2	6.342(4)	7.551(4)	6.051(5)	92.14(3)					
	178.2	6.353(4)	7.552(4)	6.055(5)	92.12(3)	β	91.42(5)	12.8(7)	−5.0(3)	4
III	188.2	7.022(2)		6.080(2)						
	198.2	7.033(2)		6.090(2)		a	6.773(30)	1.32(15)		29
	208.2	7.044(2)		6.101(2)						
	213.2	7.056(2)		6.113(2)		c	5.843(33)	1.25(16)		36
	217.2	7.058(3)		6.118(3)						
II	219.2[b]	7.060(4)		6.124(4)						
I	218.2[c]	8.632(6)								
	219.2[b]	8.627(8)								
	223.2	8.645(6)				a	8.244(23)	1.79(9)		14
	228.2	8.653(7)								
	233.2	8.661(6)								
	238.2	8.669(6)								

[a] T is in Kelvins. β is in degrees. a, b, c, and p_0-p_2 are in angstroms. R is the reliability factor. [b] Coexistence between phases II and I. [c] Undercooled phase I.

molecular interactions. Therefore, the principal coefficients of the thermal-expansion tensor correspond to the weakest and strongest interactions in the crystal structure. On the basis of this simple and well-known idea, the intermolecular interactions of TBCl have been analyzed in phases IV, III and I, where the tensor has been determined.

To account for the relative degree of intermolecular interactions, the tensor of the lowest-temperature phases II ($P2_1/m$) and I ($P4/n$) of TBCN have also been determined. Unfortunately, other structures concerning *tert*-butyl compounds have not been determined to date, and thus, a global correlation cannot be done.

To determine the thermal-expansion tensor of TBCl, several patterns were collected for each phase at different temperatures (seven for phase IV and six each for phases III and I). After the patterns were indexed, lattice parameters were refined by means of the AFMAIL program[37] at each temperature. The refined lattice parameters were fitted as a function of the temperature using a standard least-squares method for each parameter. Table 4 gathers the determined lattice parameters as well as the coefficients of the polynomial equations. The reliability factor, defined as $R = (\sum(y_o - y_c)^2/y_c^2)$, where y_o and y_c are the measured and calculated lattice constants, respectively, has been used to estimate the agreement between them and is included in Table 4. The variation of the lattice parameters as a function of temperature is depicted in Figure 5 for the different phases.

Concerning the determination of the tensor of TBCN, the experimental lattice parameters were obtained from a previous work.[9] In this case, 13 measurements were performed in the lowest-temperature monoclinic phase II from 5 to 232 K, and 11 were performed for the highest-temperature tetragonal phase I, from 234 to 285 K. The polynomial equations corresponding to the fitted lattice parameters as a function of the temperature are summarized in Table 5.

The deformation of the lattice dU due to a small temperature variation dT can be expressed by a second-rank tensor (α_{ij}), $du_{ij} = \alpha_{ij}dT$. The procedure and the method of determining the principal coefficients as well as the direction of the principal axes of the tensor have been published elsewhere.[27,41] The program DEFORM[42] was used for the calculation of the tensor.

Phase IV of TBCl and Phase II of TBCN. The tensor of a monoclinic lattice is defined by the principal coefficients (α_i, $i = 1-3$) and for an angle between the direction of one of the principal directions (α_1 in this case) and the crystallographic axis a, with the α_3 axis being coincident with the binary b axis of the lattice. Figure 6 depicts the evolution of the principal coefficients of the thermal-expansion tensor as a function of the temperature for TBCl and TBCN. In the measured low-temperature region of TBCl, the three principal coefficients reach similar values (about 10^{-4} K^{-1}), and thus, the thermal-expansion tensor is rather isotropic. Nevertheless, such isotropy takes place at lower temperatures in the case of TBCN. When the temperature is increased, the principal coefficient α_1 moves away (increasing the anisotropy of the deformation) in both cases. Figure 7 shows a three-dimensional plot of the isobaric thermal-expansion tensor in the frame of the principal axes $\alpha_1-\alpha_3$, together with the direction of the crystallographic axes. The molecular dipole direction is also included. As can be inferred from Figure 6, the deformation in the α_1 direction is the highest ("soft" direction) and corresponds closely to the [100] crystallographic direction in phase IV of TBCl as well as in phase II of TBCN. In addition, the lowest deformation corresponds to the (100) plane ("hard" plane). In the case of TBCN, the α_2 direction (close to [001] crystallographic direction) is even negative (contraction) in the highest temperature range of phase II. Such anisotropy in the principal coefficients means that the intermolecular interactions joining the molecules of both TBCl and TBCN are highly anisotropic. As it has been stated previously in the analysis of the structures of phase IV for TBCl and in previous works for phase II of TBCN,

(41) Chanh, N. B.; Clastre, J.; Gaultier, J.; Haget, Y.; Meresse, A.; Lajzerowicz, J.; Filhol, A.; Thomas, M. *J. Appl. Cryst.* **1988**, *21*, 10.
(42) Filhol, A.; Lajzerowicz, J.; Thomas, M. *DEFORM program*; unpublished software, 1987.

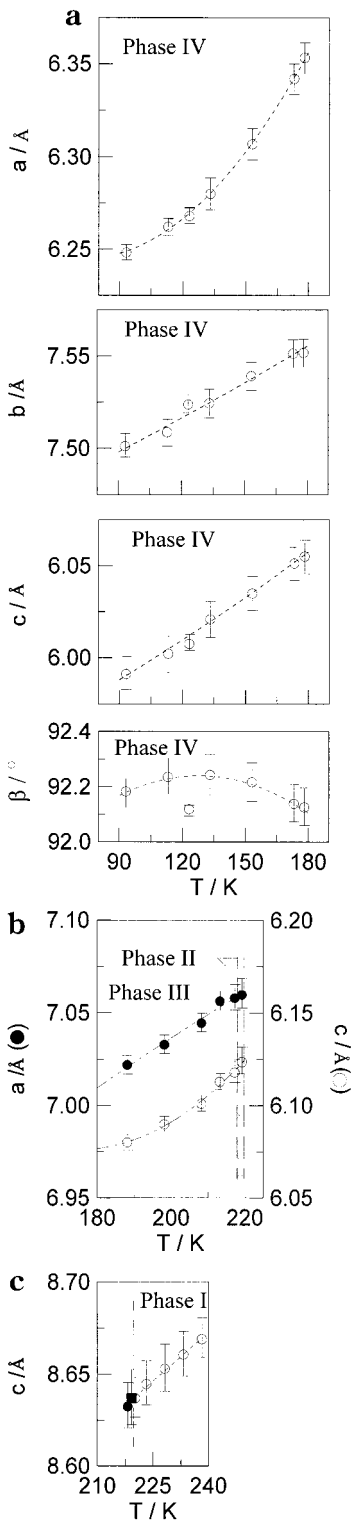

Figure 5. Lattice parameters of TBCl for phases IV (a), III (b), and I (c). In Figure 5c, ■ corresponds to the parameter for the measurement coexisting phases II and I and ● for the undercooled phase I.

the dipolar axes of the molecules (C'_3) are very close to the *c* crystallographic direction, then producing the highest intermolecular interactions in this direction. It must be pointed out that the packing in the [001] crystallographic direction is quite similar in both compounds. With this line of reasoning, it can be straightforward concluded that the differences in the *c* parameter between both compounds (about 0.7 Å for the whole

Table 5. Lattice Parameters Corresponding to the Phases II and I of TBCN together with the Polynomial Equation[a] $p = p_o + p_1T + p_2T^2$ to which They Were Fitted

phase	parameter	p_o	$p_1 \times 10^3$	$p_2 \times 10^5$	$R \times 10^4$
II	*a*	6.120(16)	−1.36(27)	0.69(10)	20
	b	6.880(17)	0.40(28)	0.04(1)	20
	c	6.722(14)	0.22(24)	0.1(1)	18
	β	95.6(2)	0.70(3)	−5.6(1)	18
I	*a*	6.481(36)	1.5(1)		10
	c	6.547(51)	0.9(2)	14	

[a] *T* is in Kelvin. p_0−p_2 are in angstroms. *R* is the reliability factor between the measured and the calculated unit-cell parameters.

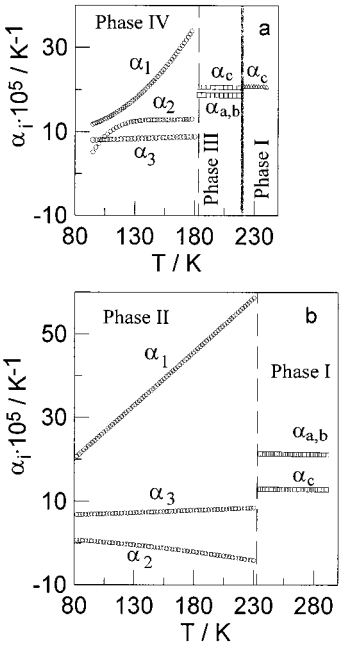

Figure 6. α_i principal coefficients as a function of temperature for TBCl (a) and TBCN (b). α_3 is chosen parallel to the crystallographic direction *b* in the monoclinic phases.

temperature range of phases IV for TBCL and II for TBCN) corresponds to the difference in the length of the molecules along their dipolar axes. Such a difference is calculated as follows: (i) for TBCl, 1.76 Å for the C−Cl bond, plus 1.78 Å for the van der Waals atomic radius of Cl atom, gives 3.54 Å. (ii) For TBCN, 1.54 and 1.16 Å for the C−C and C−N bonds, respectively, plus 1.55 Å for the van der Waals radius of N atom, give 4.25 Å, with the difference then being ca. 0.7 Å.

The (001) crystallographic plane corresponds to the plane where the rotation about the C'_3 molecular axis takes place. Moreover, the intermolecular distances in such a plane correspond to *a* and *b* lattice parameters, with *a* being shorter than *b* whatever the temperature is. The temperature increase of the frequency of the reorientations about the C'_3 axis between identical positions causes the molecules to move further apart in the direction close to the *a* crystallographic direction (particularly, the α_1 direction). Along the [010] crystallographic direction, this effect does not exist because the nearest neighbors are more widely separated. Such a result, which is stated for both compounds, is clearly shown in the three-dimensional plot of the thermal-expansion tensor (Figure 7).

Phase III of TBCl and Phase I of TBCN. According to the Newmann principle, the thermal-expansion tensor

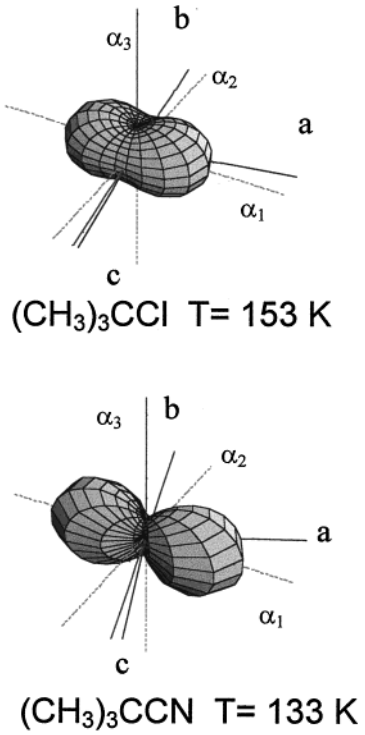

Figure 7. Thermal-expansion tensors of phases IV of TBCL at $T = 153$ K and II of TBCN at $T = 133$ K in the frame of the principal directions $\alpha_1-\alpha_3$ (dotted red line) together with the crystallographic axes $a-c$ (continuous blue line). The molecular dipoles (green lines) are also included. The full length of the α_i axes corresponds to 10^{-3} K^{-1}.

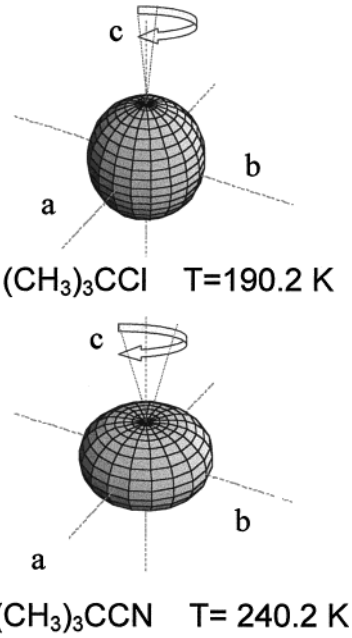

Figure 8. Thermal-expansion tensors of phases III of TBCl at $T = 190.2$ K and I of TBCN at $T = 240.2$ K in the frame of the principal directions $\alpha_a-\alpha_c$ that are coincident with the crystallographic axes $a-c$. The molecular dipoles performing the librational motions around c axis are included (green lines). The full length of the α_i axes corresponds to 10^{-3} K^{-1}.

has to display the point group symmetries of the crystal. The principal axes are coincident with crystallographic axes ($\alpha_{a,b}$, α_c). Therefore, the 4-fold axis of the tetragonal phases III of TBCl and I of TBCN is taken as the α_c direction of the thermal-expansion tensor. Figure 8 displays the three-dimensional plot of the tensors corresponding to the tetragonal phases of both compounds. In addition to the anisotropy produced by the lattice symmetry in both cases, the comparison of the principal coefficients along the [001] and [100] (or the equivalent [010]) crystallographic directions provides additional evidence of the intermolecular interactions that were predicted early in the case of TBCN.[8] The head-to-tail arrangement of the two molecules of the tetragonal unit cell produces the highest intermolecular interactions in the [001] direction in the case of TBCN (α_c direction) and the lowest in the (001) plane (see Figure 6b). On the contrary, such a situation is inverted in the case of TBCl; i.e., the highest intermolecular interaction is displayed in the (001) plane (see Figure 6a). Such an a priori nonevident result can easily be explained with the help of the molecular dynamics considerations. Concerning the [001] direction, the associated principal coefficient (α_c) is smaller for TBCN (about 12×10^{-5} K^{-1}) than for TBCl (about 20.6×10^{-5} K^{-1}). This fact means that the intermolecular interaction in the former is higher than in the latter, the reason being 2-fold: (i) On one hand, the dipole of TBCN molecule (3.65 D) is considerably higher than that of TBCl (2.1 D), a fact that was also taken into account for the monoclinic phases. (ii) On the other hand, the reorientations about the C'_3 axis are accompanied by small fluctuations about 10−15° of that axis (librational motions), which have been found to be strongly cooperative by using neutron scattering methods.[8] In the case of TBCl, only a small fluctuations of a few degrees of the dipolar axis were found (see Figure 8). Moreover, it must be pointed out that the difference between c parameters of phases III of TBCl (about 6.1 Å) and I for TBCN (about 6.7 Å) is smaller than the difference of the length of the molecules. Thus, stearic hindrance along the c crystallographic direction must produce the mentioned strong correlations.

As far as the thermal-expansion tensor in the (001) plane is concerned ($\alpha_a = \alpha_b = \alpha_{a,b}$; see Figure 6), the principal coefficients in such a plane are quite similar in both TBCN and TBCl tetragonal structures (about 21×10^{-5} and 18×10^{-5} K^{-1}, respectively). Once again, the increase in the frequency of the librational motions related with the C'_3 axis can be assumed to be the responsible for the higher deformation of TBCN, where the molecules are more tilted (10−15°) and closer ($a = b = 6.85$ Å) than for those for TBCl (few degrees and $a = b = 7.05$ Å, respectively). The arrows in Figure 8 depict the fluctuations of the C'_3 axes around the crystallographic direction c.

Phase I of TBCl. The fcc phase I of TBCl corresponds to an orientationally disordered phase where overall molecular reorientation is present. From the lattice parameter (about 8.65 Å), it can be seen that the nearest-neighbor distance is about 6.12 Å, which is almost the same as that of the c parameter of phase III. So then, the isotropic intermolecular interactions in phase I are produced by the same effects as that in the [001] direction of phase III, giving rise to similar principal coefficients. Figure 6a shows clearly the similarity between the principal coefficients in the (001) plane of phase III ($\alpha_{a,b}$) and the coefficients of phase I ($\alpha_a = \alpha_b = \alpha_c = \alpha_{a,b,c}$).

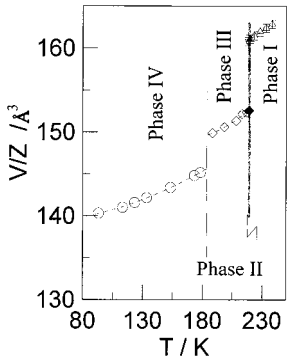

Figure 9. Volume occupied by a molecule in the solid-state phases of TBCl as a function of temperature: ○, phase IV; ◇, phase III; △ phase I; filled symbols correspond to the tetragonal phase II and fcc phase I coexisting; and ▽, undercooled phase I.

Table 6. Volume Changes ΔV (cm^3 mol^{-1}) at the Phase Transitions from Our X-ray Data, from *PVT* Data[10] and the Clausius−Clapeyron Equation Applied to the *P*−*T* Equilibrium Curve[25] with ΔH of This Work

transition data	IV−III	III−II/I	I−L
X-ray data	2.4	5.0	4.6
PVT data[10]	1.8	4.4	4.6
P−*T* slope[25]	2.0	4.5	4.4

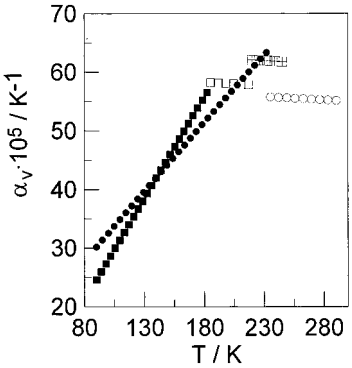

Figure 10. Volume expansivity (α_v) as a function of the temperature for phases IV (■), III (□), and I (⊞) of TBCl and II (●) and I (○) of TBCN.

Volume Changes at the Phase Transitions. Figure 9 displays the volume per molecule of the unit cell for the different phases of TBCl. From the extrapolation of these X-ray diffraction data at the temperature of the transitions, the volume change can be evaluated. Table 6 displays the determined volume changes from our X-ray data as well as those obtained by means of *PVT* measurements.[10] The volume changes have been also calculated by assuming the slope of the *P*−*T* equilibrium curve from Wenzel and Schneider[25] and the enthalpy changes of the present work. Despite the evident differences, the values from X-ray diffraction data are in reasonable agreement with those calculated from the calorimetric data. It must be pointed out that values obtained from *PVT* data are generally more accurate due to the possibility to take into account the pretransitional effects. Surprisingly, the melting transition, for which pretransitional effects become generally more marked, displays the closer values.

Volume Expansivity (α_v) and Aspherism Coefficient. Figure 10 shows the variation of the volume expansivity (α_v) of the studied compounds with the temperature for all of the phases. Concerning the monoclinic phases of

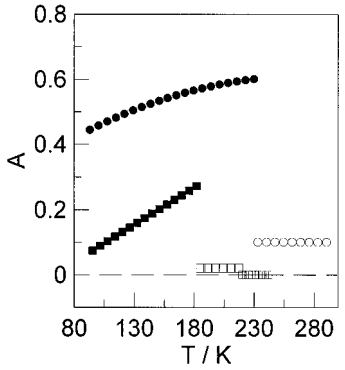

Figure 11. Aspherism index (*A*) as a function of the temperature for phases IV (■), III (□), and I (⊞) of TBCl and II (●) and I (○) of TBCN.

TBCN and TBCl, we can see a continuous increasing of the α_v parameter, which is governed by the deformation in the α_1 direction ("soft" direction) corresponding to the [100] crystallographic direction in each phase (phase IV for TBCl and phase II for TBCN). Concerning tetragonal phases, the α_v value of phase III for TBCl is higher than that corresponding to phase I of TBCN, as a consequence of the lowest intermolecular interaction along the *c* direction, which is controlled by the dipolar interactions.

It is quite obvious that the analysis of the volume expansivity wholly neglects the details of the intermolecular interaction anisotropy. To account for such anisotropy, an aspherism index has been defined as

$$A = (^2/_3)[1 - (3\beta/\alpha_v^2)]^{1/2}$$

where $\beta = \alpha_1\alpha_2 + \alpha_2\alpha_3 + \alpha_1\alpha_3$.[43] The variation of the aspherism index for TBCl and TBCN with temperature is depicted in Figure 11. The aspherism index of both monoclinic TBCl and TBCN increases with temperature as a consequence of the increase in the anisotropy of the intermolecular interactions. Moreover, such anisotropy is, in the whole temperature range of the monoclinic phases, higher for TBCN than for TBCl, a direct consequence of the higher intermolecular interaction in the [001] direction, and smaller in the (001) plane in TBCl than in TBCN.

Concerning tetragonal phases, it has been concluded in a previous section that the intermolecular interactions in the (001) plane are quite similar in both TBCN and TBCl whereas the strong difference in the dipole moment makes a sizable difference in the [001] direction. So then, the anisotropy of phase I of TBCN is considerably higher than that of TBCl.

Finally, it is quite evident that according to the cubic symmetry of phase I of TBCl the thermal-expansion tensor of this phase is isotropic ($A = 0$).

4. Conclusions

The polymorphic behavior of TBCl has been analyzed in the light of new crystallographic as well as thermal measurements.

The low-temperature phase IV of TBCl has been determined to be $P2_1/m$, and the comparison with phase

(43) Weigel, D.; Beguemsi, T.; Garnier, P.; Gerad, J. F. *J. Solid State Chem.* **1978**, *23*, 241.

II of TBCN has enabled us to establish that both compounds are isostructural.

Concerning phase II, the narrow temperature domain, roughly established previously,[17] has been confirmed (from 217.9 to 219.8 K) by means of C_p measurements. The lattice symmetry of phase II is considered to be tetragonal according to the similarity of its X-ray diffraction pattern with that of phase III.

Finally, the intermolecular interactions in the solid-state phases of TBCl have been analyzed in terms of the thermal-expansion tensor. Comparison to the thermal-expansion tensor of TBCN for phases II and I has also been performed in order to evaluate the interactions that control the stability of the structures. For the monoclinic ($P2_1/m$) phases (IV for TBCl and II for TBCN), the soft direction was found to be close to the [100] crystallographic direction, with the hard plane being the (100) direction as a consequence of the dipolar configuration and the disorder around the molecular dipole axis (3-fold rotation). The thermal expansion of tetragonal phases (III for TBCl and I for TBCN) are slightly modified due to the librational motions corresponding to the fluctuations of the dipolar axes.

For the strictly speaking unique orientationally disordered phase (I) of TBCl, the (isotropic) intermolecular interactions are controlled by the same effects as those in the [001] direction of the tetragonal phase III.

Acknowledgment. The authors are grateful to the DGE for the financial support (Grants PB95-0032 and APC1998-0123).

CM9911565